Nucleon-nucleon short-range wave function and hard bremsstrahlung $pp \to pp\gamma$

N. A. Khokhlov,[1] V. A. Knyr,[1] V. G. Neudatchin,[2,*] and A. M. Shirokov[2]
[1]*Khabarovsk State Technical University, Tikhookeanskaya 136, Khabarovsk RU-680035, Russia*
[2]*Skobeltsyn Institute of Nuclear Physics, Moscow State University, RU-119899 Moscow, Russia*
(Received 28 March 2000; published 29 September 2000)

Various opportunities to investigate the short-range NN wave function are discussed, having in mind, in particular, the quark degrees of freedom. It is shown that hard bremsstrahlung in the process $pp \to pp\gamma$ at proton beam energies of 350–500 MeV discriminates efficiently pp-wave functions with the short-range nodes in S and P waves that correspond to the Moscow potential of the NN interaction and wave functions obtained with repulsive core mesonic potentials. In the regions of maximal photon energies in the c.m. system (it means forward and backward photon emission angles in the laboratory frame) the $pp \to pp\gamma$ cross section calculated with the Moscow potential has maxima which are 3–5 times larger in comparison to that for repulsive core mesonic potentials. The analyzing power A_y is calculated too, but it is not very sensitive to the kind of NN potential used. The coordinate representation formalism of the bremsstrahlung theory is exposed.

PACS number(s): 13.75.Cs, 03.65.Nk, 12.39.Jh, 25.20.Lj

I. INTRODUCTION

The problem of quark degrees of freedom in the NN system and in the lightest nuclei was vigorously discussed in the literature from the 1970s up to now [1–16].

Initially, calculations for the six-quark system by using the resonating group method (RGM) with the perturbative one-gluon-exchange qq interaction [4–11] have shown that, albeit the resulting NN interaction may conceptually be due to mechanisms other than meson exchange, it pragmatically appears to be close—for example, in fitting phase shifts in the energy region $E_{lab} \leqslant 500$ MeV—to the interaction that is described by so-called repulsive core potentials (RCPs). This is because of the superposition of peripheral NN attraction associated with the excited quark configuration $s^4p^2[42]_X[42]_{CS}$ (which was first introduced in Ref. [3]) and short-range repulsion due to the configuration $s^6[6]_X[2^3]_{CS}$ (Ref. [1]). Later, similar conclusions were obtained [12–15] using nonperturbative models of, say, instanton-induced qq interactions. However, such views do not find some more or less evident support in the current QCD lattice calculations [17].

Recently, some new insight into the origin of the short-range NN interaction has appeared [16] based on the Glozman-Riska model of baryon structure [18]. This model explains quantitatively for the first time the excitation spectra of three kinds of baryons (N, Δ, and Λ) supposing a linear quark confinement and flavor-spin exchange between constituent quarks by means of pseudoscalar mesons.

In Ref. [16] RGM calculations result in a short-range repulsion between nucleons, albeit the physical round being very different in comparison to both the picture of gluon- or instanton-induced qq interactions [4–15] and the traditional picture of meson-exchange potentials (composite nucleon, no vector mesons, etc.). However, the nucleon-nucleon system may have its important specific features not very visible in the baryonic spectra (say, the big confinement fluctuations in the nucleon-nucleon overlap region connected with the virtual color exchange between nucleons).

As a summary of the aforesaid, there are different model views of the NN interaction and the inavoidable radical simplifications inherent to models should be verified by the proper experiments.

It was noted in Refs. [19,20] that the nature of the short-range part of the NN interaction can be disclosed to an essential degree by extending considerably (up to E_{lab} values of 5–6 GeV) the energy region in which NN scattering is analyzed. For comparison, one of the most advanced versions of RCP—the πNN coupled channel model [21]—describes the NN scattering data rather well up to E_{lab} values about 2 GeV (but also the $pp \to pp\eta$ reaction near threshold, etc. [21]).

Analysis of data on NN scattering in the wide energy range mentioned above, together with a direct investigation of the behavior of the NN wave function at small distances, enables an important verification of a concept [2,3,6,19,20,22,24] that is an alternative to the RCP approach, the concept of a deep attractive potential that involves forbidden states and which yields an NN wave function having oscillations in S and P waves instead of short-range suppression due to the repulsive core. This NN potential, referred to as the Moscow potential (MP), can find its microscopic ground in the excited quark configurations s^4p^2 and s^3p^3 for S and P waves, respectively [2,3,22]. Such configurations may predominate in the overlap region of two nucleons due to several reasons: a strong color-magnetic interaction of the $\lambda\lambda\sigma\sigma$ symmetry between quarks with the resulting energetically favorable configuration $s^4p^2[42]_X[42]_{CS}$ (Refs. [3,6]); a strong instanton-induced interaction between quarks of $\tau\tau\sigma\sigma$ symmetry with the corresponding configuration $s^4p^2[42]_X[42]_{TS}$ (Refs. [2,12]); virtual color exchange between nucleons represented by the virtual decay $s^4p^2[33]_C \to s^2p[21]_C + s^2p[21]_C$ of the six-quark colorless system to two color dipoles with strong short-range attraction between them [24].

The introduction of the MP has offered the opportunity to explain [19,20] for the first time the general features of the

*Electronic address: neudat@nucl-th.npi.msu.su

angular dependences of the differential cross sections and polarizations for NN scattering in the energy range $0<E_{lab}<6$ GeV (a new phase shift analysis of NN scattering extended up to the E_{lab} value of 2.5 GeV [25] can be very helpful here to refine the rising with energy role of absorption, etc.). A specific implementation of this approach also made it possible to describe the NN system at low and intermediate energies better (and in a rather simple way) than in the RCP approach [22,23].

So the opportunity to discriminate two kinds of NN potentials with very different short-range behavior seems rather actual. Namely, with the aid of hard electromagnetic processes we can verify whether the wave function develops bright short-range oscillations in the S and P waves (with the nodes at 0.5 and 0.9 fm, respectively) which are characteristics of local Moscow potential [19,22,23] or these oscillations are suppressed in part due to, say, the very nonlocal nature of the NN interaction [9,11] or they are suppressed completely in accordance with RCP prescriptions. There are two possibilities for such an investigation. The first (most obvious one) is associated with the deuteron-photodisintegration process $^2\mathrm{H}+\gamma\rightarrow n+p$, but the implementation of this possibility requires photon energies E_γ in excess of 1.5 GeV to suppress the strong screening effect of meson exchange currents (MECs). First experimental results obtained in this field will be analyzed elsewhere.

In this study, we consider the second possibility, the investigation of hard bremsstrahlung in the process $pp\rightarrow pp\gamma$ at proton-beam energies of several hundred MeV, whose experimental implementation is much simpler. This process was studied experimentally in coplanar geometry at energies between 42 and 280 MeV [26–28] and at 390 and 730 MeV [29] (but the photons in Ref. [29] were not hard enough). Theoretical calculations for this reaction were performed in Refs. [26,30–36]. In these calculations, attention was focused on a comparison of various RCPs—in particular, on the possibilities of tracing the differences in relevant off-energy-shell scattering amplitudes in order to make thereby a choice between these potentials, which are nearly equivalent on the energy shell (i.e., give nearly the same phase shift). The result was discouraging [36] because the distinctions proved so small that they can hardly be detectable experimentally (the general comment justifying this pessimistic conclusion from the viewpoint of meson field theory was also given in Ref. [36]). In addition, it was established that the net contribution of MECs (associated with the virtual transition $\rho,\ \omega\rightarrow\pi^0+\gamma$) and of an intermediate Δ isobar is insignificant if the hardest possible photons are considered [36–38] and can therefore be disregarded.

Introducing the MP as a potential that is radically different from RCPs in the region of short distances we demonstrate here that the process $pp\rightarrow pp\gamma$ provides a highly sensitive tool for choosing between the above two types of NN interactions. A sufficient degree of sensitivity is achieved at proton-beam energies of about 350–500 MeV (with the registration of hard photons), which are accessible at many laboratories of the world. Previously, the calculation of the reaction $pp\rightarrow pp\gamma$ with the MP was performed only by Fearing [33], who considered energies that are insufficiently high for revealing distinctions between the $pp\rightarrow pp\gamma$ cross sections as predicted with the RCPs and MP.

The formal origin of the high discriminating power of the $pp\rightarrow pp\gamma$ process is connected with the fact that the MP and RCPs are not phase-shift-equivalent potentials, as far as the S matrix corresponding to the MP has very different structure in comparison to that for RCPs: in channels with the orbital momenta $L=0$ and 1 it has extra poles (reflecting the deeply bound forbidden states) and the phase shifts are positive in the entire energy region. Namely, at small energies (up to $E_0\approx 400-500$ MeV) the S- and P-phase shifts for the MP can be obtained approximately from these for RCPs by the displacement up on 180°; at higher energies their comparative behavior becomes rather different and finally at energies of 5 GeV they have the common Born limit $|\delta_L(E)|\ll 1$.

Another possible example of such high discriminating power is the reaction of quasielastic knockout of protons by a few GeV electrons $^2\mathrm{H}(e,e'p)n$ but the measurements should be extended up to the large recoil momentum values $q\geqslant 1$ GeV/c. The quite measurable enhancement of the proton momentum distribution in deuterons for the MP in comparison with that for RCPs is expected here [a very strong final state NN interaction is the specific characteristics of the MP and at the analysis of the experiment it should be taken into account by means of the full distorted-wave impulse approximation (DWIA) procedure].

For the sake of completeness, it should be noted that there is one more method for studying quark degrees of freedom in the NN system and its wave function at small distances. This independent (albeit less direct) method, which requires, however, as the reaction $^2\mathrm{H}(\gamma,p)n$ does, much higher energies than the process $pp\rightarrow pp\gamma$, involves investigating the baryon-baryon (BB) content of the deuteron [39]. The point is that the quark configuration $s^4p^2[42]_X[42]_{CS}$ is projected, with a large amplitude (in the nucleon-overlap region of radius about 0.7 fm), not only onto the $n+p$ channel but also onto other BB channels. This is, above all, the $NN^*(1/2^-,3/2^-)$ channel with P-wave relative motion (the probability of this channel was predicted to be slightly below 1% of the probability of the $n+p$ channel, for which normalization to unity is dominated by the volume outside the nucleon-overlap region), but the N^*N^* and NN^{**} ($1/2^+$ Roper resonance) components with S-wave relative motions are not negligible either. The presence of the NN^* component with P-wave relative motion of nucleons is just suggested by the results of polarization experiments (at Dubna) that employed 7 GeV deuterons to study elastic backward scattering in the $d+p$ system [40] and inclusive reactions of the type $A(d,p)X$ with a spectator proton emitted in the forward direction [41] (a possible subprocess featuring this component is that in which N^* belonging to the deuteron and having an orbital angular momentum equal to unity is picked up by the proton, forming thereby a deuteron). According to these experiments, the probability of the NN^* component in the deuteron is around 2%, which is a remarkable argument in favor of our quark views [39]. Another possible way of studying the BB content of the deuteron could be analysis of the spectrum of spectator baryons B from the quasielastic proton knockout $^2\mathrm{H}(e,e'p)B$ at

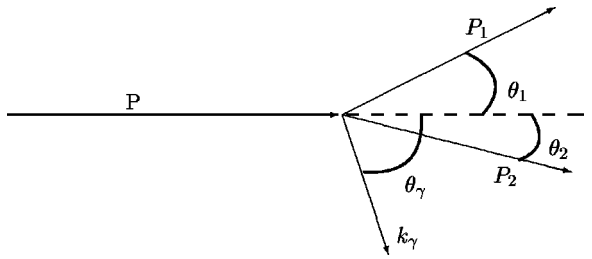

FIG. 1. Kinematic variable in the reaction $pp \to pp\gamma$ for coplanar geometry.

electron energies of 5 GeV and energies of emitted protons of the order of 2 GeV [39,42,43]. It is expedient to perform such experiments at the Thomas Jefferson National Laboratory.

We begin our analysis of the process $pp \to pp\gamma$ by giving an outline of the formalism that we employ.

II. THEORETICAL FORMALISM

We consider bremsstrahlung from the pp system in coplanar geometry, which was used in the experiments reported in Refs. [26–29]. In these studies, the experimental procedure consisted in detecting all three final particles in coincidence and involved determining the proton emission angles Θ_1 and Θ_2 in the laboratory frame and the photon emission angle Θ_γ. The protons are emitted on different sides of the beam axis, and the angle Θ_γ is reckoned in the same direction as the angle Θ_2 (see Fig. 1). The angles Θ_1, Θ_2, and Θ_γ completely determine the kinematics of the above coplanar process. Knowing these angles and the incident-proton momentum p, we can calculate, in the laboratory frame, the final-proton momenta p_1 and p_2, the photon energy ε_γ, and other quantities.

All calculations were performed in the coordinate representation. The pp-wave function was sought by solving numerically the Schrödinger equation with a relevant potential of the NN interaction and with allowance for the Coulomb interaction of protons. Such an approach is more complicated than the momentum-space one, having in mind the calculation of matrix elements of electromagnetic transitions for wave functions with Coulomb asymptotic behavior. In the process $pp \to pp\gamma$, the Coulomb interaction is operative for maximally hard photons, in which case two final protons are virtually stopped in the c.m. system (c.m.s.) However, an advantage of our approach is that, in both initial and final states, the pp-wave functions in a continuum are automatically orthogonal to forbidden states. Such states must be especially eliminated in order that a correct off-energy-shell scattering amplitude be obtained from momentum-space calculations with potentials involving forbidden states.

We do not take into account MECs, whose contribution is presumably negligible for the hardest photons (the role of MECs is comprehensively discussed in Refs. [36–38]). We calculated the wave functions of the relative motion of nucleons on the basis of the nonrelativistic Schrödinger equation; however, in going over from the laboratory frame to the c.m.s., we employed relativistic Lorentz transformations. This approach was used in a number of studies (see, for example, Refs. [30–34]). Various relativistic corrections to it were also investigated, and it was shown (see, for example, Refs. [34,44]) that they are of the order 25–30 %.

It should be borne in mind, however, that, following photon emission, the momentum of the center of mass of two final protons differs from the momentum of the center of mass of two initial protons; hence, the emitted photon has different energies in these two reference frames. These distinctions are noticeable when the emitted photons are rather hard. We performed all calculations both in the c.m.s. of the initial protons and in the c.m.s. of the final protons, and the results proved different, as they must in the nonrelativistic approach. It seems that the two values obtained for the cross section specify a reasonable interval for the true cross section. We will see below that these distinctions may be noticeable, but they are always less than the spread of the results that stems from performing calculations with NN interactions of different types.

In coplanar geometry, the $pp \to pp\gamma$ cross section is given by the expression [31] (we use the system of units in which $\hbar = c = 1$)

$$d\sigma = \left[\frac{p_1^2 p_2^3}{(2\pi)^5 32 m p \epsilon_1 [p_2^2(\epsilon_\gamma + \epsilon_2) + \epsilon_2 \vec{p}_2 \cdot (\vec{p}_1 - \vec{p})]} \times \frac{dp_1}{d\theta_\gamma} d\theta_\gamma d\Omega_1 d\Omega_2 \right] |A_{i \to f}|^2, \quad (1)$$

which must be summed over the spin states of the final protons and averaged over the spin states of the initial protons if we are not interested in polarization observables. In the above expression, $\vec{p}$ and ε are the three-momentum and energy of the incident proton; $\vec{p}_1$, $\vec{p}_2$ and ε_1, ε_2 are three-momenta and energies of the final protons, $\varepsilon_i = p_i^2/2m$; $\vec{k}$ and ε_γ are the momentum and energy of the emitted photon; and m is the proton mass. The kinematic factor in the brackets is invariant under Lorentz transformations; it can be calculated in the laboratory frame. To evaluate $dp_1/d\theta_\gamma$ we can then use the relation

$$\frac{dp_1}{d\theta_\gamma} = [p_2 \epsilon_1 (x_1 + x_2 + x_3) + \epsilon_1 \epsilon_2 (y_1 + y_2)] z^{-1}, \quad (2)$$

where

$$z = -p_1 \epsilon_2 (\sin\theta_\gamma - \tan\theta_2 \cos\theta_\gamma) + p_2 \epsilon_1 (\sin\theta_\gamma - \tan\theta_1 \cos\theta_\gamma) \frac{\cos\theta_1}{\cos\theta_2} - \epsilon_1 \epsilon_2 (\tan\theta_2 - \tan\theta_1) \cos\theta_1,$$

$$x_1 = p_1 \frac{(\sin\theta_\gamma - \tan\theta_1 \cos\theta_\gamma)(\cos\theta_\gamma + \tan\theta_2 \sin\theta_\gamma) \cos\theta_1}{(\sin\theta_\gamma - \tan\theta_2 \cos\theta_\gamma) \cos\theta_2},$$

$$x_2 = p\frac{(\sin\theta_\gamma - \tan\theta_1\cos\theta_\gamma)(\cos\theta_\gamma + \tan\theta_2\sin\theta_\gamma)}{(\sin\theta_\gamma - \tan\theta_2\cos\theta_\gamma)(\tan\theta_1 - \tan\theta_2)\cos\theta_2\tan\theta_2},$$

$$x_3 = k\frac{(\cos\theta_\gamma + \tan\theta_1\sin\theta_\gamma)(\sin\theta_\gamma - \tan\theta_2\cos\theta_\gamma)}{(\tan\theta_1 - \tan\theta_2)\cos\theta_2},$$

$$y_1 = -p_1(\tan\theta_2 - \tan\theta_1)\frac{(\cos\theta_\gamma + \tan\theta_2\sin\theta_\gamma)\cos\theta_1}{(\sin\theta_\gamma - \tan\theta_2\cos\theta_\gamma)},$$

$$y_2 = p\tan\theta_2\frac{(\cos\theta_\gamma + \tan\theta_2\sin\theta_\gamma)}{(\sin\theta_\gamma - \tan\theta_2\cos\theta_\gamma)}.$$

The squared modulus of the amplitude $A_{i\to f}$ in Eq. (1) is also a Lorentz-invariant quantity. This enables us to calculate it in the c.m.s. of two protons by using the relativistic wave functions $\varphi_i(\vec{r})$ and $\varphi_f(\vec{r})$ of the relative motion of nucleons in the initial and final states, respectively. With the aid of the standard QED method [45], we can represent $A_{i\to f}$ in the form (see Appendix)

$$A_{i\to f} = 16(\pi)^3\sqrt{\pi}m\left(\frac{e}{im}\vec{M}^{el} + \mu\,{}^1\vec{M}^{mag} + \mu\,{}^2\vec{M}^{mag}\right)\cdot\vec{\varepsilon}, \tag{3}$$

$$\vec{M}^{el} = \int d^3r[\exp(-i\vec{k}\cdot\vec{r}/2) - \exp(i\vec{k}\cdot\vec{r}/2)] \times[\overline{\varphi_f(\vec{r})}\vec{\nabla}\varphi_i(\vec{r}) - \varphi_i(\vec{r})\vec{\nabla}\overline{\varphi_f(\vec{r})}], \tag{4}$$

$${}^1\vec{M}^{mag} = \int d^3r\,\overline{\varphi_f(\vec{r})}[\vec{k}\times(\vec{\sigma}_1 + \vec{\sigma}_2)]\varphi_i(\vec{r}) \times[\exp(-i\vec{k}\cdot\vec{r}/2) + \exp(i\vec{k}\cdot\vec{r}/2)], \tag{5}$$

$${}^2\vec{M}^{mag} = \int d^3r\,\overline{\varphi_f(\vec{r})}[\vec{k}\times(\vec{\sigma}_1 - \vec{\sigma}_2)]\varphi_i(\vec{r}) \times[\exp(-i\vec{k}\cdot\vec{r}/2) - \exp(i\vec{k}\cdot\vec{r}/2)]. \tag{6}$$

In the expressions, the bar over the final-state wave function $\varphi_f(\vec{r})$ denotes Hermitian conjugation, e and μ are the proton charge and magnetic moment, the Pauli matrices $\vec{\sigma}_i$ act on the spin variables of the ith proton, and $\varepsilon = (0,\vec{\varepsilon})$ is the photon polarization four-vector (in the transverse gauge used here, we have $\vec{\varepsilon}\cdot\vec{k} = 0$). The matrix element $\vec{M}^{el}$ is associated with the proton electric charge, while the matrix elements ${}^1\vec{M}^{mag}$ and ${}^2\vec{M}^{mag}$ are generated by the particle magnetic moment. The matrix elements $\vec{M}^{el}$ and ${}^1\vec{M}^{mag}$ are associated with transitions that conserve the total spin S of the two-proton system, whereas the matrix element ${}^2\vec{M}^{mag}$ describes spin-flip transitions.

The two-proton system may be in one of two states with a definite value of the total spin S. These are the singlet ($S=0$) and triplet ($S=1$) states. The corresponding wave functions of the continuum spectrum are written as [46,47]

$$\varphi^{s(\pm)} = \varphi^{(\pm)}(\vec{p},\vec{r};0,0) = \sqrt{\frac{2}{\pi}}\frac{1}{pr}\sum_{l=0}^{\infty}{}^{even}\sum_{m=-l}^{l} i^l u_l^{(\pm)}(p,r)\mathcal{Y}_{lm}(\hat{r})\mathcal{Y}^*_{lm}(\hat{p})\chi_{oo} \tag{7}$$

for the singlet state and as

$$\varphi^{t(\pm)} = \varphi^{(\pm)}(\vec{p},\vec{r};1,\mu_i) = \sqrt{\frac{2}{\pi}}\frac{1}{pr}\sum_{j=0}^{\infty}\sum_{l'=|j-1|}^{j+1\,odd}\sum_{l=|j-1|}^{j+1\,odd}\sum_{M=-j}^{j}\sum_{m=-l}^{l}\sum_{m'=-l'}^{l'}\sum_{\mu=-1}^{1} i^{l'}u^{j(\pm)}_{l',l}(p,r)\mathcal{C}^{jM}_{lm\,1\mu_i}\mathcal{C}^{jM}_{l'm'\,1\mu}\mathcal{Y}_{l'm'}(\hat{r})\mathcal{Y}^*_{lm}(\hat{p})\chi_{1\mu} \tag{8}$$

for the triplet state. In the above expression, $\vec{p}$ and $\vec{r}$ are the relative momentum and coordinate of the particles, $\chi_{S\mu}$ is the spin component of the wave function, $\mathcal{C}^{lm}_{l_1m_1\,l_2m_2}$ are Clebsch-Gordan coefficients, and $\mathcal{Y}_{lm}(\hat{x})$ are the spherical harmonics of the unit vector $\hat{x}$ directed along the vector $\vec{x}$.

The asymptotic expression for the initial-state (final-state) wave function $\varphi_i(\vec{r}) = \varphi^{s,t(+)}$ ($\varphi_f(\vec{r}) = \varphi^{s,t(-)}$) of the continuous spectrum must be represented as the sum of the plane and diverging (converging) spherical waves. The solutions with these properties are constructed by solving the radial Schrödinger equation with the corresponding boundary conditions in the asymptotic region for the radial wave functions $u_l^{(\pm)}(p,r)$ and $u^{j(\pm)}_{l',l}(p,r)$ in the singlet and triplet states, respectively. For the initial state, these boundary conditions are given by

$$u_l(p,r) = u_l^{(+)}(p,r) \xrightarrow[r\to\infty]{} e^{i(\eta_l+\delta_l)} \times\sin\left(pr - \frac{l\pi}{2} - \xi\ln 2pr + \eta_l + \delta_l\right), \tag{9}$$

$$u^j_{l',l}(p,r) = u^{j(+)}_{l',l}(p,r) \xrightarrow[r\to\infty]{} (-i)^{l'}\frac{i}{2}\{(-1)^l\delta_{ll'} \times\exp[-i(pr - \xi\ln 2pr)] - S^j_{l',l}e^{2i\eta_l}\exp[i(pr - \xi\ln 2pr)]\}, \tag{10}$$

where we have used standard conventions (see, for example, Ref. [47]). The final-state radial wave functions $u_l^{(-)}(p,r)$ and $u^{j(-)}_{l',l}(p,r)$ are complex conjugates of the corresponding initial-state wave functions.

The formulas for computing the components $(\vec{M}^{el})_\mu$, $({}^1\vec{M}^{mag})_\mu$, and $({}^2\vec{M}^{mag})_\mu$ of the vector amplitudes $\vec{M}^{el}$, ${}^1\vec{M}^{mag}$, and ${}^2\vec{M}^{mag}$ of the reaction $pp\to pp\gamma$ are obtained by replacing the initial- and final-state wave functions $\varphi_i(\vec{r})$ and $\varphi_f(\vec{r})$ in Eqs. (4)–(6) by expressions (7) and (8) and by expanding the plane waves $\exp(\pm i\vec{k}\vec{r}/2)$ appearing in Eqs. (4)–(6) into series in terms of spherical harmonics. The resulting expressions, in which the z axis is chosen along the photon momentum $\vec{k}$ to simplify the presentation, are given below for various types of transitions separately.

A. Singlet-singlet transitions

The matrix elements of singlet-singlet transitions involve only the electric component

$$
\begin{aligned}
(\vec{M}^{el}_{(S=0\to S=0)})_\mu = &-\frac{8}{\pi}\sum_{l_i,l_f=0}^{even}\sum_{m_i=-l_i}^{l_i} i^{l_i-l_f+L}\mathcal{Y}^*_{l_i m_i}(\hat{p}_i)\mathcal{Y}_{l_f(m_i-\mu)}(\hat{p}_f)\\
&\times\Bigg[\sum_{L=|l_i-1-l_f|}^{|l_i-1+l_f|\,odd}(2L+1)\mathcal{C}^{l_f\,m_i-\mu}_{l_i-1\;m_i-\mu\;L0}\mathcal{C}^{l_f 0}_{l_i-1\;0\;L0}\mathcal{C}^{l_i m_i}_{l_i-1\;m_i-\mu\;1\mu}\sqrt{\frac{(2l_i-1)l_i}{(2l_f+1)(2l_i+1)}}\\
&\times\int_0^\infty dr\frac{2}{k}\hat{j}_L(kr/2)\frac{u_{l_f}(p_f,r)}{p_f}\left(\frac{d}{dr}+\frac{l_i+1}{r}\right)\frac{u_{l_i}(p_i,r)}{p_i r}-\sum_{L=|l_i+1-l_f|}^{|l_i+1+l_f|\,odd}(2L+1)\mathcal{C}^{l_f\,m_i-\mu}_{l_i+1\;m_i-\mu\;L0}\\
&\times\mathcal{C}^{l_f 0}_{l_i+1\;0\;L0}\mathcal{C}^{l_i m_i}_{l_i+1\;m_i-\mu\;1\mu}\sqrt{\frac{(2l_i+3)(l_i+1)}{(2l_f+1)(2l_i+1)}}\int_0^\infty dr\frac{2}{k}\hat{j}_L(kr/2)\frac{u_{l_f}(p_f,r)}{p_f}\left(\frac{d}{dr}-\frac{l_i}{r}\right)\frac{u_{l_i}(p_i,r)}{p_i r}\Bigg].
\end{aligned}
$$

Here and in the formulas given below, $\hat{j}_l(x)$ is the Riccati-Bessel function [48], and $\vec{p}_i$ and $\vec{p}_f$ are the momenta of the relative motion of the nucleons in the initial and final states, respectively.

B. Triplet-triplet transitions

The electric component has the form

$$
\begin{aligned}
(\vec{M}^{el}_{(S=1,\mu_i\to S=1,\mu_f)})_\mu = &-\frac{8}{\pi}\sum_{j_i,j_f=0}^{\infty}\sum_{M_i=-j_i}^{j_i}\sum_{M_f=-j_f}^{j_f}\sum_{l_i'=|j_i-1|}^{j_i+1\,odd}\sum_{l_f'=|j_f-1|}^{j_f+1\,odd}\sum_{l_i=|j_i-1|}^{j_i+1\,odd}\sum_{l_f=|j_f-1|}^{j_f+1\,odd}\sum_{m_i'=-l_i'}^{l_i'}\sum_{m_f'=-l_f'}^{l_f'}\sum_{m_i=-l_i}^{l_i} i^{l_i-l_f+L}\mathcal{Y}^*_{l_i' m_i'}(\hat{p}_i)\\
&\times\mathcal{Y}_{l_f' m_f'}(\hat{p}_f)(-1)^{m_f'+m_i-\mu}\mathcal{C}^{j_i M_i}_{l_i'\;m_i'\;1\;\mu_i}\mathcal{C}^{j_i M_i}_{l_i\;m_i\;1\;\mu}\mathcal{C}^{j_f M_f}_{l_f'\;-m_f'\;1\;\mu_f}\mathcal{C}^{j_f M_f}_{l_f\;-m_i+\mu\;1\;\mu}\\
&\times\Bigg[\sum_{L=|l_i-1-l_f|}^{|l_i-1+l_f|\,odd}(2L+1)\mathcal{C}^{l_f\,m_i-\mu}_{l_i-1\;m_i-\mu\;L\;0}\mathcal{C}^{l_f\,0}_{l_i-1\;0\;L\;0}\mathcal{C}^{l_i\,m_i}_{l_i-1\;m_i-\mu\;1\;\mu}\sqrt{\frac{(2l_i-1)l_i}{(2l_f+1)(2l_i+1)}}\\
&\times\int_0^\infty dr\frac{2}{k}\hat{j}_L(k/2)\frac{u^{j_f}_{l_f,l_f'}(p_f,r)}{p_f}\left(\frac{d}{dr}+\frac{l_i+1}{r}\right)\frac{u^{j_i}_{l_i,l_i'}(p_i,r)}{p_i r}-\sum_{L=|l_i+1-l_f|}^{|l_i+1+l_f|\,odd}(2L+1)\mathcal{C}^{l_f\,m_i-\mu}_{l_i+1\;m_i-\mu\;L\;0}\\
&\times\mathcal{C}^{l_f\,0}_{l_i+1\;0\;L\;0}\mathcal{C}^{l_i\,m_i}_{l_i+1\;m_i-\mu\;1\;\mu}\sqrt{\frac{(2l_i+3)(l_i+1)}{(2l_f+1)(2l_i+1)}}\int_0^\infty dr\frac{2}{k}\hat{j}_L(kr/2)\frac{u^{j_f}_{l_f,l_f'}(p_f,r)}{p_f}\left(\frac{d}{dr}-\frac{l_i}{r}\right)\frac{u^{j_i}_{l_i,l_i'}(p_i,r)}{p_i r}\Bigg].
\end{aligned}
$$

The magnetic component is given by

$$
\begin{aligned}
&({}^1\vec{M}^{mag}_{(S=1,\mu_i\to S=1,\mu_f)})_\mu \\
&=\frac{8\sqrt{2}}{\pi}(\delta_{\mu,1}-\delta_{\mu,-1})k \\
&\times\sum_{j_i,j_f=0}^{\infty}\sum_{M_i=-j_i}^{j_i}\sum_{M_f=-j_f}^{j_f}\sum_{l_i'=|j_i-1|}^{j_i+1\,odd}\sum_{l_f'=|j_f-1|}^{j_f+1\,odd}\sum_{l_i=|j_i-1|}^{j_i+1\,odd}\sum_{l_f=|j_f-1|}^{j_f+1\,odd}\sum_{m_i=-l_i}^{l_i}\sum_{m_f=-l_f}^{l_f}\sum_{m_i'=-1}^{1}\sum_{m_f'=-1}^{1}\sum_{\mu_i'=-1}^{1}\sum_{\mu_f'=-1}^{1}\sum_{L=|l_i-l_f|}^{|l_i+l_f|\,even} i^{l_i-l_f+L+1} \\
&\times(2L+1)\mathcal{Y}^*_{l_i'm_i'}(\hat{p}_i)\mathcal{Y}_{l_f'm_f'}(\hat{p}_f)(-1)^{m_f'+m_f}\mathcal{C}^{j_iM_i}_{l_i'm_i'1\mu_i}\mathcal{C}^{j_iM_i}_{l_im_i1\mu_i'}\mathcal{C}^{j_fM_f}_{l_f'-m_f'1\mu_f}\mathcal{C}^{j_fM_f}_{l_f-m_f1\mu_f'}\mathcal{C}^{l_fm_f}_{l_im_iL0}\mathcal{C}^{l_f0}_{l_i0L0}\mathcal{C}^{1\mu_f'}_{1\mu_i'1\mu}\sqrt{\frac{(2l_i+1)}{(2l_f+1)}} \\
&\times\int_0^\infty dr\frac{u^{j_f}_{l_f,l_f'}(p_f,r)}{p_f}\frac{2}{kr}\hat{j}_L(kr/2)\frac{u^{j_i}_{l_i,l_i'}(p_i,r)}{p_i}.
\end{aligned}
$$

C. Singlet-triplet and triplet-singlet transitions

The matrix elements of these spin-flip transitions involve only the magnetic components

$$
\begin{aligned}
({}^2\vec{M}^{mag}_{(S=0\to S=1,\mu_f)})_\mu &=-\frac{8}{\pi}(\delta_{\mu,1}-\delta_{\mu,-1})k\sum_{j_f=0}^{\infty}\sum_{l_i=0}^{\infty\,even}\sum_{M_f=-j_f}^{j_f}\sum_{l_f'=|j_f-1|}^{j_f+1\,odd}\sum_{l_f=|j_f-1|}^{j_f+1\,odd}\sum_{m_f=-l_f}^{l_f}\sum_{m_f'=-l_f'}^{l_f'}\sum_{m_i=-l_i}^{l_i}\sum_{L}^{odd} i^{l_i-l_f+L+1}(2L+1) \\
&\times\mathcal{Y}^*_{l_im_i}(\hat{p}_i)\mathcal{Y}_{l_fm_f}(\hat{p}_f)\mathcal{C}^{j_fM_f}_{l_f'm_f'1\mu_f}\mathcal{C}^{j_fM_f}_{l_fm_f1\mu}\mathcal{C}^{l_fm_f}_{l_im_iL0}\mathcal{C}^{l_f0}_{l_i0L0}\sqrt{\frac{(2l_i+1)}{(2l_f+1)}} \\
&\times\int_0^\infty dr\frac{u^{j_f}_{l_f,l_f'}(p_f,r)}{p_f}\frac{2}{kr}\hat{j}_L(kr/2)\frac{u_{l_i}(p_i,r)}{p_i}, \\
({}^2\vec{M}^{mag}_{(S=1,\mu_i\to S=0)})_\mu &=\frac{8}{\pi}(\delta_{\mu,1}-\delta_{\mu,-1})k\sum_{j_i=0}^{\infty}\sum_{M_i=-j_i}^{j_i}\sum_{l_i'=|j_i-1|}^{j_i+1\,odd}\sum_{l_i=|j_i-1|}^{j_i+1\,odd}\sum_{m_i=-l_i}^{l_i}\sum_{l_f=0}^{\infty\,even}\sum_{mi'=-l_i'}^{l_i'}\sum_{m_f=-l_f}^{l_f}\sum_{L}^{odd} i^{l_i-l_f+L+1}(2L+1) \\
&\times\mathcal{Y}^*_{l_i'm_i'}(\hat{p}_i)\mathcal{Y}_{l_fm_f}(\hat{p}_f)\mathcal{C}^{j_iM_i}_{l_i'm_i'1\mu_i}\mathcal{C}^{j_iM_i}_{l_im_i1-\mu}\mathcal{C}^{l_fm_f}_{l_im_iL0}\mathcal{C}^{l_f0}_{l_i0L0}\sqrt{\frac{(2l_i+1)}{(2l_f+1)}} \\
&\times\int_0^\infty dr\frac{u_{l_f}(p_f,r)}{p_f}\frac{2}{kr}\hat{j}_L(kr/2)\frac{u^{j_i}_{l_i,l_i'}(p_i,r)}{p_i}.
\end{aligned}
$$

In dealing with the matrix elements $\vec{M}^{el}$, ${}^1\vec{M}^{mag}$, and ${}^2\vec{M}^{mag}$, the most serious difficulties are encountered in calculating the integrals involving the radial wave functions of the continuous spectrum. Following Ref. [49], we calculate such integrals numerically within the interaction region and analytically outside it.

Analyzing power $A_\alpha(\alpha=x,y,z,)$ is described by the well-known formula

$$
A_\alpha=\frac{T_r[(\vec{\sigma}\cdot\vec{n}_\alpha)A_{i\to f}\overline{A}_{i\to f}]}{T_r[A_{i\to f}\overline{A}_{i\to f}]}, \tag{11}
$$

with [32]

$$
\begin{aligned}
A_x&=(T^2_{12}+T^2_{21})/(T^2_{11}+T^2_{22}),\\
A_y&=i(T^2_{12}-T^2_{21})/(T^2_{11}+T^2_{22}),\\
A_z&=(T^2_{11}-T^2_{22})/(T^2_{11}+T^2_{22}),
\end{aligned} \tag{12}
$$

where the indices 1 and 2 above denote the spin projection m_1 value equal to $1/2^+$ and $1/2^-$, respectively, of the incident nucleon onto its momentum direction (change of basis $Sm\to m_1m_2$),

$$T^2_{ab} = \sum_{m_2 m_3 m_4} \left(\langle m_3 m_4 | \vec{M} | a m_2 \rangle \langle m_3 m_4 | \vec{M} | b m_2 \rangle^* - \frac{1}{k^2} \langle m_3 m_4 | \vec{k}\vec{M} | a m_2 \rangle \langle m_3 m_4 | \vec{k}\vec{M} | b m_2 \rangle^* \right),$$

$$\vec{M} = (\vec{M}^{el} + \tau^1 \vec{M}^{mag} + \tau^2 \vec{M}^{mag}), \quad (13)$$

$\tau = im\mu/e$, and $A_x = A_z = 0$ for coplanar geometry, vector $\vec{A} = (0, A_y, 0)$ being directed perpendicular to the proton scattering plane.

In comparison with our preliminary results [50] in the present paper the new improved version of the Moscow potential [23] is used and the exposition is complemented by the analysis of transversal analyzing power A_y. As far as the MP version [23] fits the phase shifts up to $E_0 = 400 - 500$ MeV the calculations are done for values of the beam energy of $E_0 = 280$, 350, 400, 450, and 500 MeV. However, our results for $E_0 = 500$ MeV have only qualitative meaning: our consideration is nonrelativistic, but as we shall see below, the relativistic effects for $E_0 = 500$ MeV are quite remarkable.

III. RESULTS OF THE CALCULATIONS

In discussing the process $pp \to pp\gamma$, we aim primarily at comparing our results obtained by using the deep attractive MP with the results produced by two potentials of the RCP type, the Paris [51] and Hamada-Johnston [52] potentials.

Figure 2(a) presents the calculated differential cross section, along with available experimental data, at a proton-beam energy of 280 MeV [27]. Small values of the angles Θ_1 and Θ_2 correspond to emission of the hardest photons. As the photon emission angle Θ_γ with respect to the beam direction increases, the photon energy in the laboratory frame decreases from about 240 to about 100 MeV, but the emission of photons with maximum c.m.s. energy corresponds to Θ_γ values near 0° and 180°. This is the reason why the differential cross sections develop distinct maxima—both in theoretical calculations and in experimental data—at Θ_γ values that are close to 0° and 180°.

We can see that all theoretical curves are close to one another and to experimental points, so that no discrimination can be drawn between the various potentials. A similar result was previously obtained by other authors, including Fearing [33], who performed calculations not only with the RCPs but also with the MP. The same pattern is observed at lower energies as well.

Figure 2(b) shows the analyzing power A_y as a function of Θ_γ angle calculated with the MP in reasonable agreement with experiment [27], too, but the RCPs give here also approximately the same result.

The situation drastically changes, however, when we increase the proton energy, step by step, to 350 MeV (Fig. 3), 400 MeV (Fig. 4), 450 MeV (Fig. 5), and, finally, 500 MeV (Fig. 6): the above maxima become sharp peaks in the MP results and remain modest in the calculations performed with

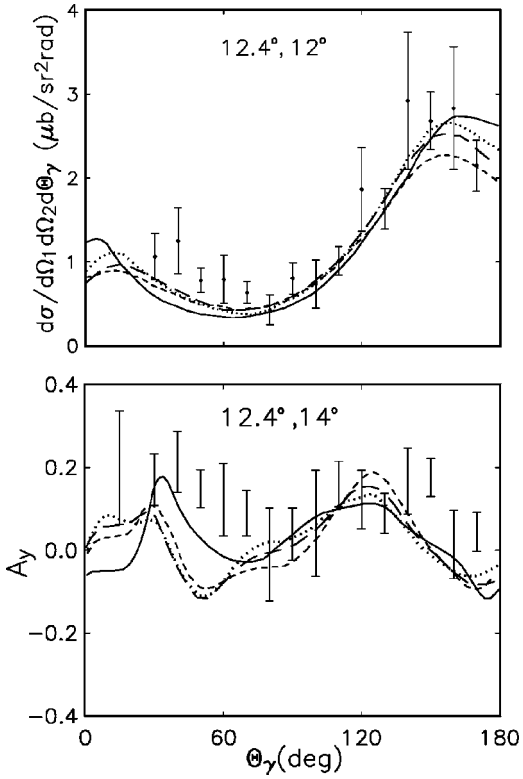

FIG. 2. (a) Differential cross section for photon emission as a function of the laboratory photon emission angle Θ_γ at proton-beam energy $\varepsilon = 280$ MeV and laboratory proton emission angles fixed at $\Theta_1 = 12.4°$ and $\Theta_2 = 12°$: solid curve, Moscow potential; dotted curve, supersymmetric partner of the MP; long-dashed curve, Paris potential; short-dashed curve, Hamada-Johnston potential. Results obtained in the c.m. systems of, respectively, initial and final protons, are practically indistinguishable. (b) Θ_γ, dependence of the analyzing power A_y at the fixed proton emission angles $\Theta_1 = 12.4°$ and $\Theta_2 = 14°$. $\varepsilon = 280$ MeV.

the RCPs. Near maxima, distinctions between the MP results obtained in the c.m. systems of the initial and final protons also manifest themselves, but these distinctions, amounting to several tens of a percent, are still less than fourfold to fivefold distinctions between the cross sections at the maxima corresponding to the MP and RCPs. It can therefore be concluded that investigation of the reaction $pp \to pp\gamma$ provides a rather promising tool for choosing between NN potentials of various types, the more so as the distinctions are seen not only in the absolute values of the cross sections but also in their shapes. It is hoped that future experiments will make it possible to make this choice.

In Figs. 2–6 the results obtained with the supersymmetric partner [53] of the MP are also presented. It belongs to the RCP family and yields the same phase shifts as the MP apart from the basic overall displacement down by π that is associated with the generalized Levinson theorem. It can be seen that the cross sections computed with the supersymmetric partner of the MP are virtually indistinguishable from the cross sections corresponding to other RCPs, albeit that some moderate difference between all of them in the prediction of the phase shift energy dependence at our energies of $E_0 = 300 - 500$ MeV does exist. In particular, Hamada-Johnston

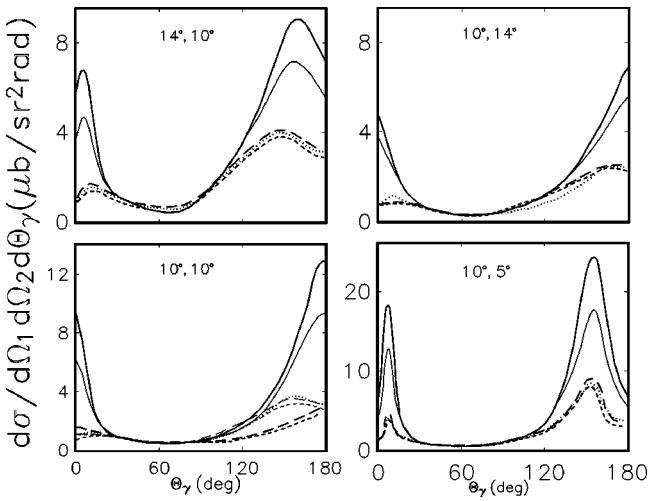

FIG. 3. The same as in Fig. 2(a) but for $\varepsilon = 350$ MeV and various values of angles Θ_1 and Θ_2 indicated in each graph. Thick lines, c.m. system of initial protons; thin lines, that of final protons (they are presented only if they are different remarkably from the corresponding thick lines).

and Paris potentials at, say, energy values around $E_{lab} = 450$ MeV produce *S*-phase shifts of *NN* scattering which differ by $10° - 15°$, but the corresponding $pp \to pp\gamma$ results are almost identical. The same conclusion is valid if we compare two versions of the MP—the last version [23] and the previous one [22,50]. Namely, in comparison with experiment, the first version [22,50] describes the singlet *D*-phase shift behavior remarkably worse than the second one [23], but the calculated $pp \to pp\gamma$ cross sections are also practically indistinguishable. So the discussed cross sections of the $pp \to pp\gamma$ reaction are not sensitive to details of the predicted phase shift running. However, they appear to be very sensitive to the type of short-range behavior of wave functions corresponding to low partial waves: the radial wave function for *S* and *P* waves with the short-range oscillations characteristic of the MP give 3–5 times larger cross section (in the maxima) than the corresponding wave functions of RCPs which are suppressed at small distances due to the repulsive core.

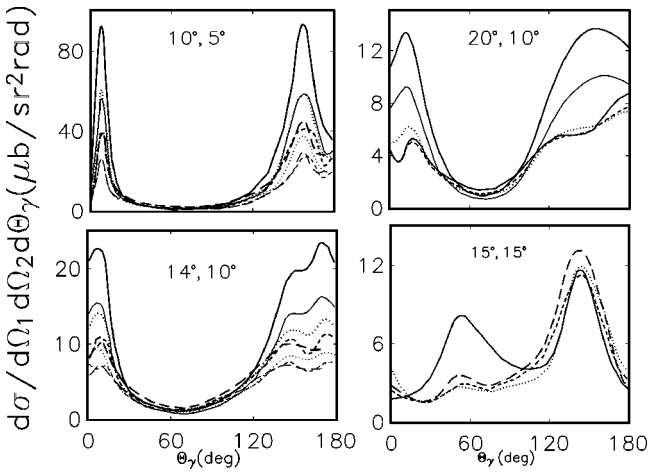

FIG. 4. The same as in Fig. 3 but for $\varepsilon = 400$ MeV.

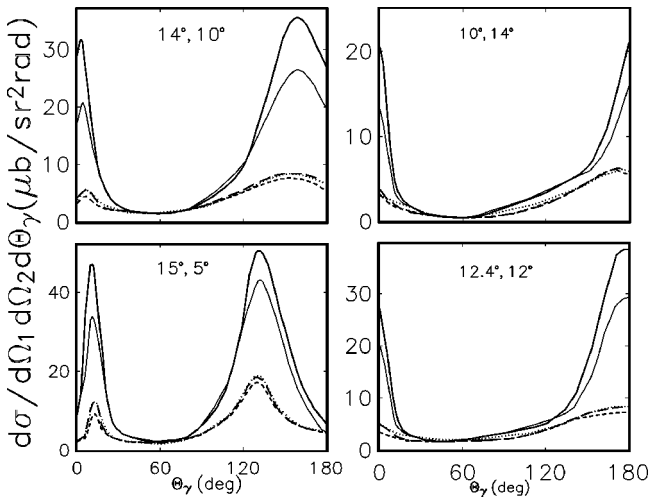

FIG. 5. The same as in Fig. 3 but for $\varepsilon = 450$ MeV.

The reason why the analysis at energies E_γ near to the maximal value will make it possible to reveal the shape of the *NN* wave function at small distances for low partial waves is that, with increasing E_γ (in the c.m.s.) and decreasing energy of the relative motion of the nucleons in the final state, the role of transitions featuring these waves becomes more pronounced (this especially concerns *S* waves).

Mathematically, the surprising sensitivity of partial-wave integrals standing in electromagnetic matrix elements to the short-range behavior of partial-wave functions has the explanation that the integrands are oscillating at large distances and the corresponding contributions to integrals are small.

Let us discuss the influence that changes in the kinematic variables exert on the cross sections computed with the MP and RCPs. Figures 3–6 show that, at the beam energies considered, an increase in photon energy E_γ, i.e., a decrease in the sum $\Theta_1 + \Theta_2$ of the proton emission angles (satisfying the condition $\Theta_1 > \Theta_2$), enhances the effect. The effect also grows in magnitude with increasing proton-beam energy at fixed Θ_1 and Θ_2.

The set of Figs. 2–6 shows also that with increasing en-

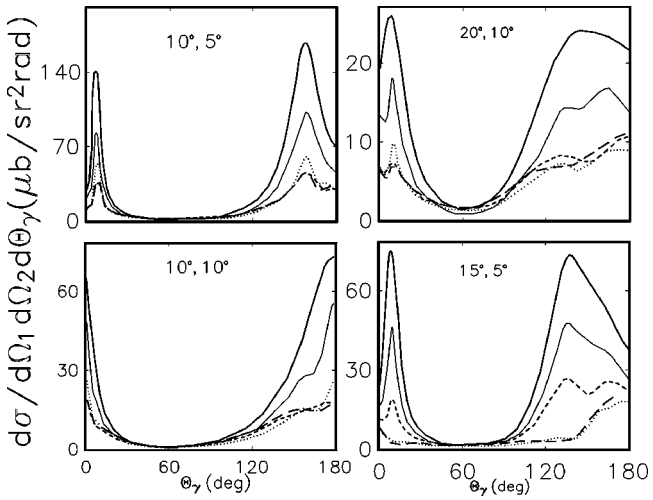

FIG. 6. The same as in Fig. 3 but for $\varepsilon = 500$ MeV.

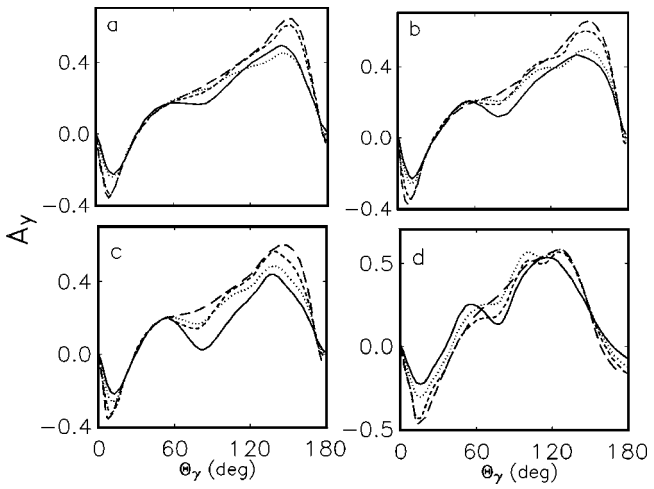

FIG. 7. $A_y(\Theta_\gamma)$, curves calculated with potentials used above for different kinematic conditions: (a) $\varepsilon=350$ MeV, $\Theta_1=14°$, $\Theta_2=10°$; (b) $\varepsilon=400$ MeV, $\Theta_1=14°$, $\Theta_2=10°$; (c) $\varepsilon=450$ MeV, $\Theta_1=14°$, $\Theta_2=10°$; (d) $\varepsilon=500$ MeV, $\Theta_1=20°$, $\Theta_2=10°$.

ergy E_0 of proton beam the difference between the results calculated in the initial c.m.s. and in the final one increases, and for $E_0=500$ MeV it becomes rather remarkable. So this energy seems a maximal one where our nonrelativistic approach still makes sense (the relativistic consideration eliminates the above difference).

To complement the data for cross sections, in Fig. 7 we present the predicted analyzing power A_y for some kinematic cases of Figs. 3–6. This quantity, as we see, being rather useful to control the spin dependence of the *NN* interaction, is not so sensitive to the kind of *NN* potential used than the differential cross sections of Figs. 2–6.

On the whole, we see that there is a kinematic region in which the excess of the cross section calculated with the MP over the one corresponding to RCPs is large. The general characteristics of this region is that the photons should be as hard as possible. Following the experimental paper in [27] we made calculations for coplanar geometry when kinematically complete information is obtained by triple coincidence measurements of three angles Θ_1, Θ_2, and Θ_γ. But it is possible also to measure in double-coincidence experiments, say, Θ_1, ε_1, and Θ_γ quantities or to use (for experimental convenience) some noncoplanar kinematics compatible with the emission of hard photons. We are ready to perform the corresponding calculations.

IV. CONCLUSION

It was noted in Refs. [33,34,36] that bremsstrahlung in the process $pp\to pp\gamma$ provides no way of distinguishing between various RCPs. In contrast to this, our study demonstrates that, even at rather moderate proton-beam energies of about 350–500 MeV, $pp\to pp\gamma$ experiments are very informative if we extend the range of *NN* potentials under comparison by confronting the MP with the RCP family. Unfortunately, experimental data on the reaction $pp\to pp\gamma$ at the required energies and kinematic conditions are not available at present. The existing data at 390 and 730 MeV [29] are characterized by relatively low photon energies.

Investigation of hard pion emission in the processes $pp\to pp\pi^0$ and $pp\to pn\pi^+$ would be a direct extension of $pp\to pp\gamma$ experiments. The quasielastic knockout reaction $^2\mathrm{H}(e,e'p)n$ can be very helpful also, if the measurements of the proton momentum distribution will be extended up to recoil momentum values of $q\sim 1$ GeV/c (with the very strong final-state *NN* interaction created by the MP taken into account in the theoretical interpretation of the data).

Heuristically, the above type of comparison of the properties of the various types of the *NN* interaction may be of broader significance, because quark microscopics behind the MP as represented here in the simplest form by the quark configuration $s^4p^2[42]_{CS}[42]_X$ is much richer in its physical content than its projection onto the *NN* channel. For this reason, we believe that the proposed method of comparison between the various models of the *NN* interaction in the reaction $pp\to pp\gamma$ would also be of interest for nonpotential approaches like RGM, which admit nonlocalities and take explicitly into account quark degrees of freedom. Analysis of the properties of the *NN* system will be more comprehensive and effective if its basis will include other reactions—for example, inclusive polarization processes featuring deuterons with energies of several GeV. It was mentioned above that, in such processes, the $NN^*(\frac{1}{2}^-,\frac{3}{2}^-)$ component with *P*-wave relative motion becomes visible in the deuteron.

ACKNOWLEDGMENTS

The authors are grateful to Prof. J.A. Eden, Prof. S.B. Gerasimov, Prof. V.I. Kukulin, Prof. J.M. Laget, Prof. Y. Mizuno, Prof. S.A. Moszkowski, Prof. I.T. Obukhovsky, Prof. V.N. Pomerantsev, and Prof N.P. Zotov for valuable suggestions and remarks. This work was supported in part by the Russian Foundation for Fundamental Research (Project No. N96-02-18072).

APPENDIX

Using the common definition of the transition amplitude $A_{i\to f}$ [45],

$$\delta(\vec{P}_i-\vec{P}_f+\vec{k})A_{i\to f} = 2\sqrt{4\pi}\int d^3x\langle\psi_f|\vec{J}(\vec{x})\vec{\varepsilon}\,|\psi_i\rangle\exp(-i\vec{k}\cdot\vec{x}), \tag{A1}$$

with photon polarization vector $\vec{\varepsilon}$ and current density

$$\vec{J}(\vec{x})=-\frac{i}{2}\sum_{i=1,2}\frac{e}{m}[\,\delta(\vec{x}-\vec{r}_i)\vec{\nabla}_i+\vec{\nabla}_i\delta(\vec{x}-\vec{r}_i)] + \sum_{i=1,2}\mu\,\mathrm{rot}\,\delta(\vec{x}-\vec{r}_i)\vec{\sigma}_i, \tag{A2}$$

we present both initial and final two-proton wave functions in the evident notation as

$$\psi(\vec{r}_1,\vec{r}_2)=(2\pi)^{3/2}\exp(i\vec{P}\cdot\vec{R})\varphi(\vec{p},\vec{r}),$$

$$\int d^3r\,\overline{\varphi}(\vec{p}_1,\vec{r})\varphi(\vec{p}_2,\vec{r})=\delta(\vec{p}_1-\vec{p}_2). \tag{A3}$$

Taking, as an example, in Eq. (A2) the component with the $\delta(\vec{x}-\vec{r}_1)\vec{\nabla}_1$ operator and substituting it into Eq. (A1) we obtain on the right-hand side the integral

$$\int d^3r_1 d^3r_2 \overline{\psi}_f(\vec{r}_1,\vec{r}_2)(\vec{\nabla}_1\cdot\vec{\varepsilon})\psi_i(\vec{r}_1,\vec{r}_2)\exp(-i\vec{k}\cdot\vec{r}_1)$$

$$=\int d^3R d^3r\,\exp(-i\vec{P}_f\cdot\vec{R})\overline{\varphi_f}(\vec{p}_f,\vec{r})\left(\frac{1}{2}\vec{\nabla}_R-\vec{\nabla}_r\right)\vec{\varepsilon}$$

$$\times\exp(i\vec{P}_i\cdot\vec{R})\varphi(\vec{p}_i,\vec{r})\exp\left[-i\vec{k}\cdot\left(\vec{R}-\frac{1}{2}\vec{r}\right)\right]$$

$$=\text{const}\left[\frac{i}{2}\vec{\varepsilon}(\vec{P}_i-\vec{k})\,\delta(\vec{P}_i-\vec{P}_f-\vec{k})\right.$$

$$\times\int d^3r\,\overline{\varphi_f}(\vec{p}_f,\vec{r})\varphi_i(\vec{p}_i,\vec{r})\exp\left(\frac{i}{2}\vec{k}\cdot\vec{r}\right)$$

$$-\delta(\vec{P}_i-\vec{P}_f-\vec{k})\int d^3r\,\overline{\varphi_f}(\vec{p}_f,\vec{r})$$

$$\left.\times(\vec{\varepsilon}\cdot\vec{\nabla}_r)\varphi_i(\vec{p}_i,\vec{r})\exp\left(\frac{i}{2}\vec{k}\cdot\vec{r}\right)\right]. \tag{A4}$$

Now, choosing, say, the initial c.m. system, i.e., $\vec{P}_i=0$, $\vec{P}_f=-\vec{k}$, we see that the first term vanishes due to the gauge condition $\vec{\varepsilon}\cdot\vec{k}=0$. If $\vec{P}_f=0$, then $\vec{P}_i=\vec{k}$ and the first term vanishes again. In this way Eq. (4) results, etc.

[1] D.A. Liberman, Phys. Rev. D **16**, 1542 (1977); C. De Tar, *ibid.* **17**, 302 (1978).

[2] V.G. Neudatchin, Yu.F. Smirnov, and R. Tamagaki, Prog. Theor. Phys. **58**, 1072 (1977).

[3] I.T. Obukhovsky, V.G. Neudatchin, Yu.F. Smirnov, and Yu.M. Tchuvil'sky, Phys. Lett. **77B**, 231 (1979).

[4] M. Harvey, Nucl. Phys. **A352**, 301 (1981).

[5] A. Faessler, F. Fernandez, G. Lubeck, and K. Shimizu, Nucl. Phys. **A402**, 555 (1983).

[6] V.G. Neudatchin, I.T. Obukhovsky, and Yu.F. Smirnov, Fiz. Elem. Chastits At. Yadra **15**, 1165 (1984) [Sov. J. Part. Nucl. **15**, 519 (1984)].

[7] V.V. Burov, V.K. Luk'yanov, and A.I. Titov, Fiz. Elem. Chastits At. Yadra **15**, 1249 (1984) [Sov. Part. Nucl. **15**, 558 (1984)].

[8] Yu.A. Svarc, Nucl. Phys. **A416**, 109 (1984); **A463**, 231 (1987).

[9] Y. Fujiwara and K.T. Hecht, Nucl. Phys. **A462**, 621 (1987).

[10] F. Myhrer and J. Wroldsen, Rev. Mod. Phys. **60**, 629 (1988).

[11] K. Shimizu, Rep. Prog. Phys. **52**, 1 (1989).

[12] M. Oka and S. Takeuchi, Phys. Rev. Lett. **63**, 1780 (1989).

[13] Z.-Y. Zhang, A. Faessler, U. Straub, and L.Ya. Glozman, Nucl. Phys. **A578**, 573 (1994).

[14] W. Koepf, L. Wilets, S. Pepin, and Fl. Stancu, Phys. Rev. C **50**, 614 (1994).

[15] D.R. Entem, A.I. Machavariani, A. Valcarce, A.J. Buchmann, A. Faessler, and F. Fernandez, Nucl. Phys. **A602**, 308 (1996).

[16] Fl. Stancu, S. Pepin, and L.Ya. Glozman, Phys. Rev. C **56**, 2779 (1997); **59**, 1219(E) (1999); Phys. Rev. D **57**, 4393 (1998).

[17] M.C. Chu, J. Grandy, S. Huang, and J. Negele, Phys. Rev. D **49**, 6039 (1994); J.W. Negele, Nucl. Phys. B (Proc. Suppl.) **73**, 92 (1999); K.F. Liu *et al.*, Phys. Rev. D **59**, 112001 (1999).

[18] L.Ya. Glozman and D.O. Riska, Phys. Rep. **268**, 263 (1996); K. Dannbom, L.Ya. Glozman, C. Helminen, and D.O. Riska, Nucl. Phys. **A617**, 555 (1997); L.Ya. Glozman, Z. Papp, W. Plessas, K. Varga, and R.F. Wagenbrunn, Phys. Rev. C **57**, 3406 (1998); L.Ya. Glozman, W. Plessas, K. Varga, and R.F. Wagenbrunn, Phys. Rev. D **58**, 094030 (1998); D.O. Riska and G.E. Brown, Nucl. Phys. **A653**, 251 (1999).

[19] V.G. Neudatchin, I.T. Obukhovsky, V.I. Kukulin, and N.F. Golovanova, Phys. Rev. C **11**, 128 (1975).

[20] V.G. Neudatchin, N.P. Yudin, Yu.L. Dorodnykh, and I.T. Obukhovsky, Phys. Rev. C **43**, 2499 (1991).

[21] T.-S.H. Lee and A. Matsuyama, Phys. Rev. C **36**, 1459 (1987); M. Batinić, A. Švarc and T.-S.H. Lee, Phys. Scr. **56**, 321 (1997).

[22] V.I. Kukulin and V.N. Pomerantsev, Prog. Theor. Phys. **88**, 159 (1992).

[23] V.I. Kukulin, V.N. Pomerantsev, A. Faessler, A. Buchmann, and E.M. Tursunov, Phys. Rev. C **57**, 535 (1998); V.I. Kukulin, V.N. Pomerantsev, and A. Faessler, Phys. Rev. C **59**, 3021 (1999).

[24] V.G. Neudatchin and I.T. Obukhovsky, in *Relativistic Nuclear Physics and QCD*, Proceedings of the XIII International Seminar, Dubna, 1994, edited by A.M. Baldin and V.V. Burov, JINR Publ. No. E1,2-97-79 (JINR, Dubna 1997), Vol. II, p. 3.

[25] R.A. Arndt, Ch.H. Oh, I.I. Strakovsky, R.L. Workman, and F. Dohrmann, Phys. Rev. C **56**, 3005 (1997).

[26] J.V. Jovanovich *et al.*, Phys. Rev. Lett. **26**, 277 (1971); D.O. Galde *et al.*, *ibid.* **25**, 1581 (1970).

[27] K. Michaelian *et al.*, Phys. Rev. C **41**, 2689 (1990).

[28] B.V. Przewoski *et al.*, Phys. Rev. C **45**, 2001 (1992).

[29] B.M.K. Nefkens, O.R. Sander, D.I. Sober, and H.W. Fearing, Phys. Rev. C **19**, 877 (1979); K. Yasuda *et al.*, Phys. Rev. Lett. **82**, 4775 (1999).

[30] V.R. Brown, Phys. Lett. **25B**, 506 (1967); Phys. Rev. **177**, 1498 (1969); V.R. Brown and J. Franklin, Phys. Rev. C **8**, 1706 (1973); V.R. Brown, P.L. Anthony, and J. Franklin, *ibid.* **44**, 1296 (1991).

[31] L. Heller and M. Rich, Phys. Rev. C **10**, 479 (1974).

[32] R.L. Workman and H.W. Fearing, Phys. Rev. C **34**, 780 (1986).

[33] H.W. Fearing, Nucl. Phys. **A463**, 95c (1987).

[34] V. Herrmann, K. Nakayama, O. Scholten, and H. Arellano, Nucl. Phys. **A582**, 568 (1995); V. Herrmann, J. Speth, and K.

Nakayama, Phys. Rev. C **43**, 394 (1991); V. Herrmann and K. Nakayama, *ibid.* **44**, R1254 (1991); **46**, 2199 (1992).
[35] M. Jetter, H. Freitag, and H. Geramb, Phys. Scr. **48**, 229 (1993); A. Katsogiannis, K. Amos, M. Jetter, and H. Geramb, Phys. Rev. C **49**, 2342 (1994); M. Jetter and H. Geramb, *ibid.* **49**, 1832 (1994).
[36] M. Jetter and H.W. Fearing, Phys. Rev. C **51**, 1666 (1995); H.W. Fearing and S. Scherer, nucl-th/9909076.
[37] J.A. Eden and M.F. Gari, Phys. Lett. B **347**, 187 (1995); Phys. Rev. C **53**, 1102 (1996).
[38] F. de Jong, K. Nakayama, V. Herrmann, and O. Scholten, Phys. Lett. B **333**, 1 (1994); F. de Jong, K. Nakayama, and T.-S. Lee, Phys. Rev. C **51**, 2334 (1995).
[39] L.Ya. Glozman, V.G. Neudatchin, I.T. Obukhovsky, and A.A. Sakharuk, Phys. Lett. B **252**, 23 (1990); L.Ya. Glozman, V.G. Neudatchin, and I.T. Obukhovsky, Phys. Rev. C **48**, 389 (1993); L.Ya. Glozman and E.I. Kuchina, *ibid.* **49**, 1149 (1994).
[40] M. Rekalo and I.M. Sitnik, Phys. Lett. B **356**, 434 (1995); L.S. Azhgirey and N.P. Yudin, in *Dubna Deuteron-97*, Proceedings of the 4th International Symposium, Dubna, 1997, edited by A.M. Baldin and S.S. Shimansky (World Scientific, Singapore, 1999), p. 97.
[41] A.P. Kobushkin, in *Proceedings of the Few-Body 14th International Conference*, Williamsburg, 1994, edited by F. Gross (CEBAF, Newport News, VA, 1994), p. 99; B. Kuehn, C.F. Perdrisat, and E.A. Strokovsky, Yad. Fiz. **58**, 1873 (1995) [Phys. At. Nucl. **58**, 1771 (1995)].
[42] J.A. Gomes Tejedor and E. Oset, Nucl. Phys. **A580**, 577 (1994).
[43] L.Ya. Glozman and A. Faessler, Phys. Lett. B **348**, 270 (1995).
[44] K.M. Liou and M.I. Sobel, Ann. Phys. (N.Y.) **72**, 323 (1972); G.H. Martinus, O. Scholten, and J.A. Tjon, Phys. Rev. C **56**, 2945 (1997).
[45] V.B. Berestetsky, E.M. Lifshitz, and L.P. Pitaevsky, *Kvantovaya elektrodinamika (Quantum Electrodynamics)* (Nauka, Moscow, 1989).
[46] M. Goldberger and K. Watson, *Collision Theory* (Wiley, New York, 1964).
[47] A.G. Sitenko, *Lektsii po teorii rasseyaniya (Lectures on Scattering Theory)* (Vishcha Shkola, Kiev, 1971).
[48] *Handbook of Mathematical Functions*, Natl. Bur. Stand. Appl. Math. Ser. No. 55, edited by M. Abramowitz and I.A. Stegun (U.S. GPO, Washington, D.C., 1965).
[49] C.M. Vincent and H.T. Fortune, Phys. Rev. C **2**, 782 (1970).
[50] V.G. Neudatchin, N.A. Khokhlov, V.A. Knyr, and A.M. Shirokov, Yad. Fiz. **60**, 1086 (1997) [Phys. At. Nucl. **60**, 971 (1997)]; N.A. Khokhlov, V.A. Knyr, V.G. Neudatchin, and A.M. Shirokov, Nucl. Phys. **A629**, 218c (1998).
[51] M. Lacombe *et al.*, Phys. Rev. C **21**, 861 (1980).
[52] T. Hamada and L.D. Johnston, Nucl. Phys. **34**, 382 (1962).
[53] D. Baye, J. Phys. A **20**, 5529 (1987); Phys. Rev. Lett **58**, 2738 (1987); F. Michel and G.Z. Reidemeister, Z. Phys. A **329**, 385 (1988).